Quasi-bound states induced by one-dimensional potentials in graphene

H. Chau Nguyen, M. Tien Hoang, and V. Lien Nguyen*
Theoretical Department, Institute of Physics, VAST, P.O. Box 429 Bo Ho, Hanoi 10000, Vietnam
(Received 14 August 2008; revised manuscript received 17 October 2008; published 20 January 2009)

We suggest a simple approach for studying the quasi-bound fermion states induced by one-dimensional potentials in graphene. Detailed calculations have been performed for symmetric double barrier structures and *n-p-n* junctions. Besides the crucial role of the transverse motion of carriers, we systematically examine the influence of different structure parameters such as the barrier width in double barrier structures or the potential slope in *n-p-n* junctions on the energy spectrum and, especially, on the resonant-level width and, therefore, the localization of quasi-bound states.

DOI: 10.1103/PhysRevB.79.035411 PACS number(s): 81.05.Uw, 73.20.At, 73.22.−f, 73.23.Ad

Over the last 3 years, graphene and graphene-based nanostructures have attracted much attention both experimentally and theoretically.[1,2] This is due to the fact that the low-energy excitations in these structures are massless chiral Dirac fermions, which behave in very unusual ways when compared to ordinary electrons in the conventional two-dimensional (2D) electron gas realized in semiconductor heterostructures. One of particularly interesting features of Dirac fermions is their insensitivity to external electrostatic potentials due to the so-called Klein paradox.[3] It seems that Dirac electrons can propagate to the hole states across a steep potential barrier without any damping.[4] In this situation, the confinement of electrons becomes quite a challenging task, while it is very important for producing the basic building blocks of electronic devices such as resonant structures, electron waveguides, or quantum dots (QDs).[1,2,5,6]

Graphene is a single layer of carbon atoms densely packed in a honeycomb lattice, which can be treated as two interpenetrating triangular sublattices often labeled by A and B. In the presence of an external electrostatic potential V, the low-energy quasi-particles of the system are formally described by the 2D Dirac-type Hamiltonian[7,8]

$$H = v_F(\vec{\sigma}\vec{p}) + mv_F^2\sigma_z + V(x,y), \tag{1}$$

where $v_F \approx 10^6$ ms^{-1} is the Fermi velocity, the pseudospin matrix $\vec{\sigma}$ has components given by Pauli matrices, and $\vec{p}=(p_x,p_y)$ is the in-plane momentum. The term mv_F^2, representing the gap in the electronic spectrum, may arise from the spin-orbit interaction,[9] from the coupling between the graphene layer and the substrate, or from the effect of covering graphene by some appropriate materials.[10,11] Eigenstates of the Hamiltonian (1) are two-component pseudospinors $\Psi=[\psi_A,\psi_B]^T$, where ψ_A and ψ_B are envelope functions associated with the probabilities at respective sublattice sites of the graphene sheet.

For one-dimensional (1D) potentials $V=V(x)$ it has been shown that the finite values of the momentum parallel to potential barrier, the transverse momentum p_y, can suppress the Klein tunneling, giving rise to the electron confinement.[12] This discovery opens a way of confining electrons and, particularly, making graphene-based homojunctions and even QDs using only electrostatic gates.[13,14] Moreover, in difference from conventional semiconductor QDs, to form a graphene-strip-based QD a single barrier seems to be sufficient.[13] Thus, 1D potentials can produce in graphene structures the quasi-bound states (QBSs), where the carriers may remain for a long (but finite) time before tunneling away. Actually,[15] each QBS can be identified by a complex energy E. Its real part Re$[E]$ defines the position of the QBS, i.e., the resonant energy level, while the imaginary part Im$[E]$ measures the width of this resonant level, which is inversely proportional to the carrier lifetime at the QBS. The smaller Im$[E]$, i.e., the shaper the resonance, the longer the carrier lifetime, i.e., the stronger the localization of QBSs becomes. Additionally, in the case when there exist in the system several QBSs, the resonant-level width should be much smaller than the interlevel spacing. So, to identify a QBS one has to determine both the resonance level position and the resonant-level width that in turn requires solving Hamiltonian (1) with appropriate boundary conditions. In this way, the Fock-Darwin states of Dirac electrons in the graphene-based QDs have been studied.[16] For a cylindrically symmetric QD, the width of QBSs was shown strongly depending on the electron angular momentum and may be as small as 1/800 compared to the interlevel spacing. For the graphene-strip-based QD induced by a parabolic 1D potential,[13] the QBSs seem to exist just inside the potential barrier (either positive or negative), whose left and right slopes work as the "tunneling barriers" for relativistic electrons (holes). Moreover, using the transmission expression semiclassically derived in Ref. 17, Silvestrov and Efetov[13] also showed an exponential decrease in quasi-bound level widths as the transverse momentum increases.

In this work, using the standard transfer (T) matrix, we suggest an approach for studying the QBSs induced by 1D electrostatic potentials in graphene. The approach is rather simple and can be in principle applied for any smooth 1D potential. As useful illustrations, the QBSs are in detail analyzed for two well-addressed graphene structures: double barrier structures[18,19] and *n-p-n* junctions.[2]

Let us consider a system described by the Hamiltonian H (1), where the confinement potential V is built along the x direction, $V \equiv V(x)$, while the motion of carriers in the y direction is assumed to be free. To extract information about QBSs, we need to impose special boundary conditions in the x direction, which means that far from the barrier the solution of H (1) should be an outgoing wave, i.e., the propagation is away from the barrier.[16] In the T-matrix

formalism, while the amplitudes of the left-to-right (C) and right-to-left (D) waves on two sides, right (r) and left (l), of the potential barrier are related to each other as $(C_r, D_r)^T = (T_{11}T_{12};\ T_{21}T_{22})(C_l, D_l)^T$, the imposed boundary conditions, implying $C_r = 0$ and $D_l = 0$, require that the element T_{22} of the (2×2) T matrix should vanish,

$$T_{22} = 0. \tag{2}$$

This is in fact the transcendental equation for determining the complex energies of QBSs. It plays the key role in the present work. Notice however that in practical calculations if we are interested only in the resonant positions we should more conveniently solve another equation, $T_{21}=0$, which exhibits only purely real solutions. This equation is resulted from the well-known expression of the transmission probability $\mathcal{T}$ in terms of T-matrix elements, $\mathcal{T} = 1 - |T_{21}|^2/|T_{22}|^2$, (see Ref. 20) and from the fact that the position of QBSs may be thought of as the resonant energy where $\mathcal{T}$ may reach the value of unity, $\mathcal{T}=1$.

Thus, following the suggested approach the problem of determining the resonant position as well as the width of QBSs consists of (i) finding the T matrix and (ii) solving Eq. (2). The advantage of T matrices is that they can easily be multiplied to build up complicated potentials in one dimension. Actually, in principle, any smooth 1D potential can be approximately treated as a series of many steep potentials, so that within each step the potential can be considered constant. The overall T matrix to be found is then simply given by multiplying the partial T matrices for all steep potentials. On the other hand, for each steep potential, the partial T matrix can be obtained from the solutions of the Hamiltonian H (1) in the left and right sides (where the potential V is constant) by requiring an appropriate condition of continuity at the steep interface. The calculating procedure is the same as in semiconductor structures,[21] but the continuity here is required only for wave functions (by matching up the corresponding amplitudes). In practice, such a procedure of constructing the overall T matrix for 1D potentials in graphene can be easily realized in computer without the need of explicitly writing down solutions of the Hamiltonian (1) for each step.

Concerning Eq. (2) for complex energies E, we would like to note that it cannot be analytically solved even for simple potentials such as rectangular barriers and double δ potentials. Fortunately, this equation seems to be easily solved numerically in the complex plane of E even for more complicated 1D potentials. To this end, we first solve the equation of purely real energy $T_{22}=0$, the solutions of which, as mentioned above, determine the energy positions of QBSs. Note that, on the other hand, the position of QBSs is also defined by the real part of the solutions of Eq. (2). Taking into account the fact that for any QBS, associated with the complex energy E, the inequality $|\mathrm{Im}[E]| \ll |\mathrm{Re}[E]|$ is always held, clearly, the solutions of the equation $T_{21}=0$ can be appropriately used as the zero-order approximation for solving Eq. (2) of complex energies E. Writing an obtained solution of Eq. (2) as $E = \mathrm{Re}[E] - i\ \mathrm{Im}[E]$, the imaginary part $\mathrm{Im}[E]$ then yields the width of the corresponding resonant level, which is hereafter denoted for short as Γ, and $\Gamma \equiv \mathrm{Im}[E]$. In this way, we have carried out numerical calculations of the position (energy spectrum) as well as the width of QBSs for two types of 1D potentials: double barrier structures and n-p-n junctions. Before showing obtained results, we notice that for Dirac electrons the most important parameter in 1D-potential problems is the transverse momentum of incident electrons $p_y = p_F \sin\varphi$, where p_F is the Fermi momentum and φ is the incident angle. Hereafter, we will for convenience deal with the transverse wave number $k_y \equiv p_y/\hbar$.[4,12]

Double barrier structure. For simplicity we will consider a symmetric double barrier structure (SDBS), where the two barriers of identical heights U and identical widths d are built along the x direction with the distance L between them (well width). Such a structure in graphene can be created by the electric field effect using a thin insulator or by local chemical doping.[4]

In the limiting case of a single quantum well (QW), when $d \to \infty$, by solving the Hamiltonian (1) Pereira *et al.*[12] calculated the energy spectrum of confined states in a large range of the transverse wave vector k_y for $mv_F^2 = 0$ and 10 meV. In this case, the T matrix can be easily constructed, which gives

$$T_{22} = e^{-\alpha}\left\{\cos\kappa - \frac{\kappa^2 + \beta^2 - \beta(f_+ + f_-)(\epsilon+\Delta) + (\epsilon+\Delta)^2}{\kappa(f_+ - f_-)(\epsilon+\Delta)}\sin\kappa\right\}, \tag{3}$$

where we use the following same symbols as in Ref. 12: $\beta = k_y L$, $\epsilon = EL/\hbar v_F$, $u = UL/\hbar v_F$, $\Delta = EL/\hbar v_F$, $\alpha = [\beta^2 - (\epsilon-u)^2 + \Delta^2]^{1/2}$, $\kappa = (\epsilon^2 - \beta^2 - \Delta^2)^{1/2}$, and $f_\pm = (\beta \pm \alpha)/(\epsilon - u + \Delta)$. With this T_{22}, after some simple algebraic transformations, we can show that Eq. (2) is exactly coincident with Eq. (9) for the energy, the key equation in Ref. 12.

In the general case of finite d, although the T matrix can still be explicitly constructed, its expression is however too lengthy to be shown. So, we will simply present numerical solutions of the energy in Figs. 1 and 2 for SDBSs with different values of d, L, and mv_F^2. The regions of semiclassical solutions, (I)–(V), separated from each other by the dashed lines in Fig. 1, have been drawn in the same way as that discussed in Ref. 12. The curves in region (II) are just the calculated energy spectrum of QBSs, plotted against the transverse wave vector k_y, for the SDBS with $U=80$ meV, $L=150$ nm, $d=100$ nm, and $mv_F^2=0$. This energy spectrum shows a qualitative similarity to that of confined states in a single QW ($d \to \infty$) reported in Ref. 12. Actually, calculations performed for SDBSs with different d, ranging from 50 to 150 nm, show only a slight difference in energy spectrum. Due to such a weak sensitivity of the energy spectrum to the barrier width d, one can speculate that the k_y dependence of resonant energies for the SDBSs considered should follow the same relation as that suggested in Ref. 12 for a single QW,

$$E_n = \hbar v_F [k_y^2 + (n\pi/L)^2]^{1/2}, \tag{4}$$

where n is an integer. This can be verified by plotting E_n^2 against k_y^2 for the SDBS with a given L, as demonstrated in

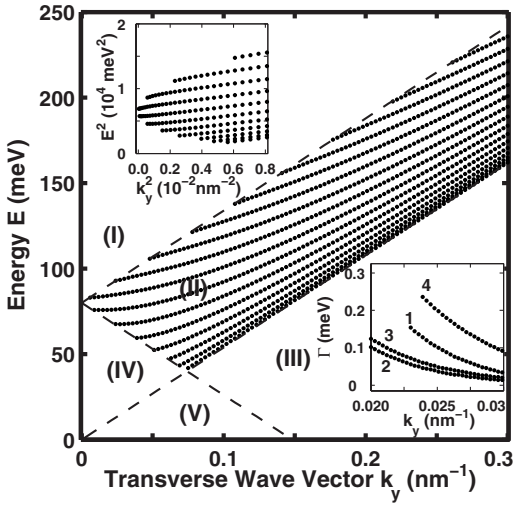

FIG. 1. Energy spectrum of QBSs in the graphene SDBS with $U_0=80$ meV, $L=100$ nm, $d=150$ nm, and $mv_F^2=0$ is plotted versus $k_y \equiv p_y/\hbar$ [lines in region (II)]. Semiclassical regions (I) free electrons, (II) QBSs, (III) forbidden, (IV) chiral tunneling, and (V) bound states (the region of free holes is not shown). The upper inset shows that $E_n^2 \propto k_y^2$ [see Eq. (4)]. The lower inset shows an exponential reduction in the resonant-level width Γ as k_y increases for the QBSs being in the considered region of k_y (the curves are numbered along the position order of the levels counted from the bottom in energy spectrum).

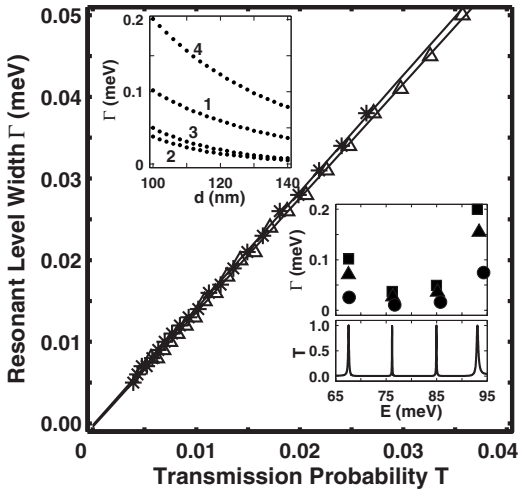

FIG. 2. Relation between the resonant-level width Γ, the transmission probability $\mathcal{T}$, and the barrier width d. The main figure shows $\mathcal{T} \propto \Gamma$ for two QBSs with smallest Γ from the upper inset [2 (*) and 3 (△)]. The upper inset shows an exponential reduction in Γ as d increases ($k_y=0.025$ nm^{-1}; the curves are numbered in the same way as in Fig. 1). In the lower inset the upper part shows effects of the energy gap [$mv_F^2=0$ (solid squares), 5 meV (solid triangles), and 10 meV (solid circles)] on the resonant position E (transverse axis) and the level width Γ (vertical axis); the lower part shows the resonant peaks in the transmission probability $\mathcal{T}$ in the case of $mv_F^2=0$ (corresponding to solid-square points in the upper part).

Fig. 1 (upper inset). Indeed, the curves fit well with the straight lines of Eq. (4) ($E_n^2 \propto k_y^2$) in the region of larger k_y when QBSs become strongly localized (as will be shown later). As for the L dependence of energies E_n, to the contrary, from the set of E_n for a great number of SDBSs with different L, ranging from 100 until 1000 nm, we still do not recognize the $E_n(L)$ relation as expected from Eq. (4). Notice that the L dependence of the energy spectrum of QBSs in graphene SDBSs is much more complicated when compared to the conventional semiconductor SDBSs. This is related to the fact that in graphene SDBSs the QBSs exist only in the energy range close to the top of barriers, so that their energy spectrum structure is very sensitive to changes of the well width L, especially for small L.

Next, we examine another basic character of QBSs, the level width Γ, which will be shown to mainly depend on the transverse momentum and the barrier width. Indeed, the lower inset in Fig. 1 demonstrates a rapid reduction in Γ as the transverse wave vector k_y increases in the region of small k_y for just the SDBS of $d=100$ nm discussed in the main figure. The upper inset in Fig. 2 shows a similar reduction in Γ, but with respect to the barrier width d, given $k_y=0.025$ nm^{-1}. Notice that for larger k_y and/or d the width Γ is too small to be shown. The observed reductions in Γ may be approximately described by the semiclassical relation $\Gamma \propto \exp[-\alpha(k_y d)]$, where however no defined value of the constant α has been recognized. Nevertheless, since the interlevel spacings only weakly vary with k_y and/or d, such a rapid reduction in Γ undoubtedly results in a strong enhancement of the localization of QBSs when the transverse wave number k_y and/or the barrier width d increases.

Further, to better understand the width Γ as that determined by the tunneling through the classically forbidden regions, for the SDBSs with different d, ranging from 100 to 140 nm, and for a given k_y ($k_y=0.025$ nm^{-1}), we have simultaneously calculated the width Γ (upper inset in Fig. 2) and the transmission probability $\mathcal{T}$ (see Ref. 20) for one of the barriers (the two barriers are identical). Then, the width Γ is plotted versus $\mathcal{T}$ as can be seen in Fig. 2 for the two states with smallest Γ (see Ref. 22) from the upper inset (lines 2 and 3, i.e., the two middle lines in the energy spectrum at the chosen value of k_y; see also the lower inset in this figure). Clearly, the data for both state-line fit well the expected linear relation $\Gamma \propto \mathcal{T}$. Hence, overall, Fig. 2 supports, for the QBSs with small level widths, the same relations between the level width Γ, the transmission probability $\mathcal{T}$, and the barrier width d, $\Gamma \propto \mathcal{T} \propto \exp[-\alpha(k_y d)]$, as those well known for the ordinary electrons in conventional semiconductor SDBSs.[21]

All the data discussed up to now are for the gapless graphene, $mv_F^2=0$. To see the gap effect we present in Fig. 2 (upper part of the lower inset) the imaginary part Im[E] (level width) versus the real part Re[E] (resonant position) of the QBS energies for SDBSs with different gap widths (see the points from top): $mv_F^2=0$, 5 and 10 meV. Comparing the three points belonging to the same resonant level in this figure, we find that while the resonant-level positions only slightly shift up, the level widths Γ considerably reduce, giving rise to an enhancement of localization of QBSs, as the gap enlarges from 0 to 10 meV. Here, notice that although the width Γ is much smaller for the two middle states, the relative reduction in Γ with respect to mv_F^2 is almost the

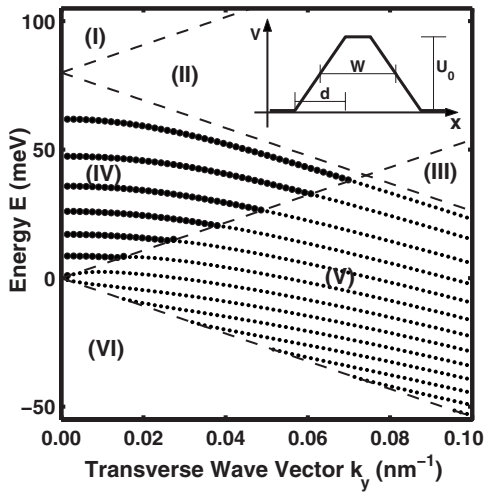

FIG. 3. Diagram of semiclassical solutions of the Hamiltonian (1) with the 1D potential $V(x)$ drawn schematically in the figure: (I) free electrons, (II) evanescent waves, (III) forbidden, (IV) (hole) QBSs, (V) bound hole states, and (VI) free holes. The lines in region (IV) show the energy spectrum of the quasi-bound hole states plotted versus k_y. These states then continuously cross over into the bound hole states with purely real energies in region (V). Inset: the potential profile $V(x)$ along the cross section of a *n-p-n* junction.

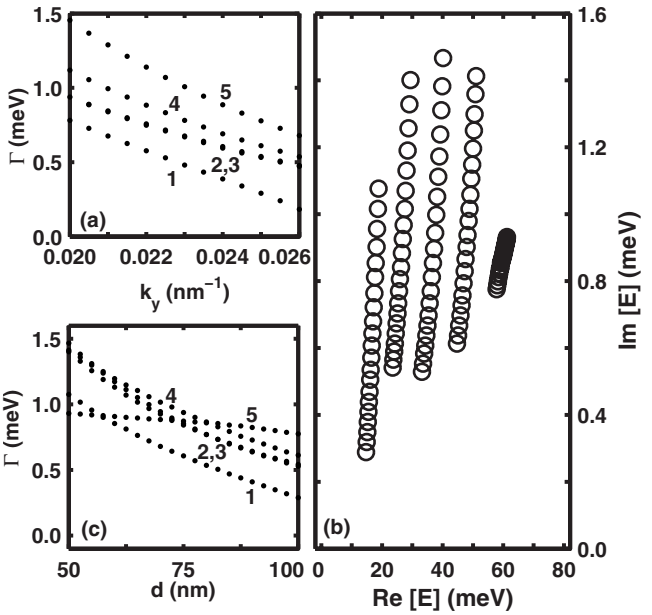

FIG. 4. Resonant-level width Γ. (a) An exponential reduction in Γ as the transverse wave vector k_y increases for the junction with $U_0=80$ meV, $W=150$ nm, and $d=100$ nm. (b) Variation in the level width (Im[E]) and the resonant position (Re[E]) as d increases from 50 nm (top) to 100 nm (bottom) ($U_0=80$ meV and $k_y=0.025$ nm^{-1}). (c) Γ from (b) is plotted versus d. The curves are numbered in the same way as in Fig. 1.

same for all the four QBSs considered. Lastly, to have an image of the resonance as well as the level width, we plot in the lower part of this inset the transmission probability $\mathcal{T}$ versus the energy E for just the case of zero gap, $mv_F^2=0$, described by the solid-square points in the upper part. Obviously, $\mathcal{T}$ has the sharp peaks at resonant energies and for each peak the full width at half maximum measures the width of corresponding level. In the cases of finite mv_F^2, the resonance peaks are much narrower.

n-p-n junction. Let us now consider the 1D-potential barrier built along the x direction as shown in Fig. 3 (inset), where the motion of electrons (holes) in the y direction is assumed to be free. This potential approximately models a *n-p-n* junction in graphene[2,23] and it is characterized by the three parameters: the barrier height (U_0), the mean barrier width (W), and the width of the *n-p* and *p-n* interfaces (d). First, in the way similar to that discussed in Refs. 12 and 13 we can qualitatively analyze the semiclassical dynamics of Dirac fermions in the potential of interest. Solutions can be then assumed consisting of six types as diagrammatically demonstrated by the regions (I)–(VI) in Fig. 3. However, we will focus in this work only on the type (IV) solution, which describes the QBSs with resonant positions defined by the condition

$$\sqrt{v_F^2\hbar^2k_y^2+m^2v_F^4} < E < U_0 - \sqrt{v_F^2\hbar^2k_y^2+m^2v_F^4} \qquad (5)$$

[region (IV) in Fig. 3]. It is readily clear from this condition that for a given U_0 the QBSs exist only in the range of small transverse wave number k_y. The basic characters of these QBSs can be now examined using the T-matrix approach.

For the potential studied, as mentioned above, the T matrix can be constructed by approximating the barrier as a series of N steep potentials along the x direction. It seems that such a calculating procedure is not only easy to be realized with a computer but also guaranteed to have a fast convergence. For example, for the barrier of $U_0=80$ meV, $W=150$ nm, and $d=100$ nm discussed below, to achieve a practically full convergent result, the number of steps N is not larger than 200. Using the obtained T matrix, we numerically solved Eq. (2) (or $T_{21}=0$ for only resonant positions as noted above) that provides the energy spectrum of QBSs (Fig. 3) as well as the resonant-level widths (Fig. 4). In region (IV) of Fig. 3, the resonant levels, appeared at small (but nonzero) k_y, slightly bend down as k_y increases that indicates the hole nature of the QBSs observed. At the same time, the width of these resonant levels, Γ, fast reduces with increasing k_y as can be seen in Fig. 4(a). An analysis shows that for typical QBSs in the middle of energy spectrum, i.e., the states 2–4 in Fig. 4(a) (see Ref. 22) the k_y dependence of Γ approximately obeys the semiclassical evaluation

$$\Gamma \propto \exp(-\pi v_F\hbar^2k_y^2d/U_0). \qquad (6)$$

As a consequence of such an exponential reduction, the width of resonant levels will quickly vanish at the boundary (dashed line in Fig. 3), where there is a continuous crossover from QBSs in region (IV) to the bound hole states (with purely real energies) in region (V) (Fig. 3). The latter region (V) is defined by the semiclassical condition

$$-[v_F^2\hbar^2k_y^2+m^2v_F^4]^{1/2} < E < \min\{[v_F^2\hbar^2k_y^2+m^2v_F^4]^{1/2}, U_0 - [v_F^2\hbar^2k_y^2+m^2v_F^4]^{1/2}\}.$$

For considered *n-p-n* junctions in graphene, the slope of potential in the *n-p* and *p-n* interface regions, measured by the magnitude of the field U_0/d, plays an exceptional role in creating QBSs of the Dirac fermions.[13,17] This is already clear in Eq. (6), where U_0/d appeared in the exponent of Γ. To learn more about the role of this parameter, we carried out calculations of E for the structures with different d, keeping U_0 fixed ($U_0=80$ nm). Certainly, in the limit of a rectangular barrier, $d\rightarrow 0$, there exists no QBSs, although the transmission probability may exhibit a weak resonance.[24] A finite d effectively induces QBSs and the larger d is then the smaller the resonant-level width of these states becomes. This can be seen in Fig. 4(b), where we plot Im[E] versus Re[E] for barriers with different d, ranging from 50 (top) to 100 nm (bottom). The figure shows that while an increase in d leads to only a slight shift down of resonant positions (Re[E]), and therefore a little variation in interlevel spacings, it causes a strong reduction in resonant-level widths (Im[E]), and consequently a strong enhancement of the localization of QBSs. The reduction in $\Gamma \equiv |\mathrm{Im}[E]|$ with increasing d can be more clearly seen in Fig. 4(c), where except curve 5, associated with the highest line in the energy spectrum, the data again roughly show the exponential dependence of Eq. (6). Notice that, for the potential studied since the left and right slopes work as the tunneling barriers, the distance d plays then the role somewhat similar to that of the barrier width in the SDBS model considered above. Both weakly influence the resonant positions, but strongly affect the resonant-level width, and therefore strongly affect the localization of QBSs. Another close correspondence can be found between the mean barrier width W in the *n-p-n* junction potential (see Fig. 3) and the well width L in the SDBS model. Both essentially define the energy spectrum structure but weakly influence the resonant-level width of QBSs.

In conclusion, we have suggested an approach for studying the QBSs induced by one-dimensional potentials in graphene. The approach is based on the standard T-matrix method and distinguished by its simplicity. Using this approach we have examined the main characters, energy spectrum and resonant-level width, of QBSs formed in two types of graphene nanostructures: double barrier structures and *n-p-n* junctions. For SDBSs with infinite barrier widths d, the T-matrix approach leads to the same equation for the energy spectrum of confined states as that reported in Ref. 12 for a single QW. For SDBSs with finite d, we have shown an exponential decrease in the resonant-level width, and therefore a strong enhancement of the localization of QBSs, when the transverse momentum and/or the barrier width increases. For the strongly localized QBSs the observed relations between the level width, the transmission probability and the barrier width are similar to those for ordinary electrons in conventional semiconductor SDBSs. For *n-p-n* junctions, we have shown the quasi-bound hole states, which exist only in the structures with a finite slope of the potential in the *n-p* and *p-n* interface regions and only in the region of small transverse momentums. It was also shown that the resonant-level width exponentially narrows and therefore the localization of QBSs is exponentially enhanced when the potential slope decreases and/or the transverse momentum increases. The potential slopes in *n-p-n* junctions play the role similar to the two barriers in SDBSs. For both structures studied the gap in electronic spectrum is one more reason for enhancing the localization of QBSs. This study of gap effect is however rather qualitative since, although the energy gap is a desired property for integrating graphene-based nanoelectronic devices, various aspects of the problem such as how to produce a gap and how the gap mutually affects other properties of material are still under discussion (see Refs. 10, 11, and 25 and references therein). Finally, it is worth mentioning that the T-matrix approach suggested is quite general and should be applicable to a wide range of 1D potentials in calculating different fundamental quantities, other than those studied in this work, such as the conductance and the noise spectrum density.

This work was supported by the Ministry of Science and Technology of Vietnam via the Program of Fundamental Researches (Project No. 4.023.06).

*nvlien@iop.vast.ac.vn

[1] A. H. Castro Neto, F. Guinea, N. M. R. Peres, K. S. Novoselov, and A. K. Geim, arXiv:0709.1163, Rev. Mod. Phys. (to be published).
[2] C. W. J. Beenakker, Rev. Mod. Phys. **80**, 1337 (2008).
[3] A. Calogeracos and N. Dombey, Contemp. Phys. **40**, 313 (1999).
[4] M. I. Katsnelson, K. S. Novoselov, and A. K. Geim, Nat. Phys. **2**, 620 (2006).
[5] C. Berger *et al.*, Science **312**, 1191 (2006).
[6] N. M. R. Peres, A. H. Castro Neto, and F. Guinea, Phys. Rev. B **73**, 241403(R) (2006).
[7] T. Ando, J. Phys. Soc. Jpn. **74**, 777 (2005).
[8] D. P. DiVincenzo and E. J. Mele, Phys. Rev. B **29**, 1685 (1984).
[9] C. L. Kane and E. J. Mele, Phys. Rev. Lett. **95**, 226801 (2005); More careful studies show a much smaller magnitude of the gap induced by the spin-orbit couplings, see D. Huertas-Hernando, F. Guinea, and A. Brataas, Phys. Rev. B **74**, 155426 (2006); H. Min, J. E. Hill, N. A. Sinitsyn, B. R. Sahu, L. Kleinman, and A. H. MacDonald, *ibid.* **74**, 165310 (2006); Y. Yao, F. Ye, X. L. Qi, S. C. Zhang, and Z. Fang, *ibid.* **75**, 041401(R) (2007).
[10] R. M. Ribeiro, N. M. R. Peres, J. Continho, and P. R. Briddon, Phys. Rev. B **78**, 075442 (2008).
[11] L. Benfatto and E. Cappelluti, Phys. Rev. B **78**, 115434 (2008).
[12] J. M. Pereira, Jr., V. Mlinar, F. M. Peeters, and P. Vasilopoulos, Phys. Rev. B **74**, 045424 (2006).
[13] P. G. Silvestrov and K. B. Efetov, Phys. Rev. Lett. **98**, 016802 (2007).
[14] B. Trauzettel, D. V. Bulaev, D. Loss, and G. Burkard, Nat. Phys. **3**, 192 (2007).
[15] D. K. Ferry and S. M. Goodnick, *Transport in Nanostructures* (Cambridge University Press, Cambridge, England, 1997).

[16] H.-Y. Chen, V. Apalkov, and T. Chakraborty, Phys. Rev. Lett. **98**, 186803 (2007).
[17] V. V. Cheianov and V. I. Falko, Phys. Rev. B **74**, 041403(R) (2006).
[18] J. M. Pereira, Jr., P. Vasilopoulos, and F. M. Peeters, Appl. Phys. Lett. **90**, 132122 (2007).
[19] R. Zhu and Y. Guo, Appl. Phys. Lett. **91**, 252113 (2007).
[20] For graphene, both electrons (with positive energies) and holes (with negative energies) can simultaneously contribute to the transmission probability at the Fermi level. Then, taking into account the chirality of Dirac carriers, the transmission $\mathcal{T}$ expressed in terms of T-matrix elements has a more complicated form covering that mentioned in the text as a particular case. This case is functioned when electron energies in the two leads have the same sign. In this work, concerning the QBSs, electron energies in both leads are positive.
[21] J. H. Davis, *The Physics of Low-Dimensional Semiconductors: An Introduction* (Cambridge University Press, Cambridge, England, 1998).
[22] For example, estimations of the ratio γ between the resonant-level width and the mean interlevel spacing give $\gamma \approx 4 \times 10^{-3}$ and 6×10^{-3} for levels 2 and 3, respectively in Fig. 2 (upper inset, $d = 100$ nm) and $\gamma \approx 6 \times 10^{-2}$ and 5×10^{-2} for levels 2 and 3, respectively, in Fig. 4(a) ($k_y = 0.025$ nm^{-1}).
[23] B. Huard, J. A. Sulpizio, N. Stander, K. Todd, B. Yang, and D. Goldhaber-Gordon, Phys. Rev. Lett. **98**, 236803 (2007).
[24] D. Dragoman and M. Dragoman, Appl. Phys. Lett. **90**, 143111 (2007); note that due to an error in calculations the result reported in this work is inaccurate. In reality, resonance is considerably weaker.
[25] S. Y. Zhou, D. Siegel, A. Federov, F. Elgabaly, A. Schmid, A. Castro Neto, and A. Lanzara, Nature Mater. **7**, 259 (2008).